This article has been accepted for publication in IEEE Transactions on Vehicular Technology. This is the author's version which has not been fully edited and content may change prior to final publication. Citation information: DOI 10.1109/TVT.2023.3289718

AI-Assisted Joint Search Approach for mmWave Cell Discovery Using Sparse MDT Data

Syed Muhammad Asad Zaidi*, Haneya Qureshi*, Marvin Manalastas*,
Adnan Abu-Dayya†, Ali Rizwan†, and Ali Imran*
*AI4Networks Research Center, University of Oklahoma-Tulsa, USA
†Department of Electrical Engineering, Qatar University, Doha Qatar
Email: {asad, haneya, marvin, ali.imran}@ou.edu, ali.rizwan@qmic.com, adnan@qu.edu.qa

***Abstract*—High signal directivity and sensitivity to blockages make the mmWave base station (BS) discovery a challenging problem in emerging mobile networks. Existing solutions include methods that rely on the exhaustive periodic beam sweeping and thus have high latency and low mmWave cell discovery rate. Joint methods where macro-BS determines the mmWave cell for a given user equipment based solely on spatial proximity are prone to Non Line of Sight (NLoS) conditions. Recent Artificial Intelligence (AI)-based solutions address the above problems but rely on impractical assumption of having complete minimization of drive test (MDT) reports traces at the assisting macro BSs in all areas of interest. This paper is the first to present an AI-based framework that can utilize very sparse MDT style data to enable NLoS-aware low latency mmWave cell discovery, hereafter referred to as AI-enabled Sparse Data based MmWave cell discOvery and EN-DC activation framework (AISMO). In AISMO framework, we first gather historic MDT traces of mmWave users containing signal strength and Radio Link Failure (RLF) indicators. We then augment this highly sparse MDT data using a variety of interpolation, domain knowledge, and AI-based techniques to create augmented mmWave coverage maps (mW-Amaps) while incorporating the NLoS conditions through the RLF traces that are inherently embedded in the data. The mW-Amaps are then used by the macro BS to determine the optimal mmWave cell for a given user location. Results show that our proposed domain knowledge-based MDT data augmentation approach, which we call Weighted Nearest Neighbor Count (WNNC), outperforms other data sparsity alleviation techniques for mW-Amap creation with accuracy of 96%. Second best in terms of accuracy is a deep learning-based solution, that has almost a 30x faster training time than the WNNC. To evaluate AISMO's performance in a realistic 5G deployment scenario, we present a case study where AISMO is used to enable E-UTRAN New-Radio Dual-Connectivity (EN-DC) between macro BS and mmWave small cells. Results show that compared to the state-of-the-art nearest mmWave BS approach that leads to 26% EN-DC activation failure due to NLoS conditions, AISMO practically offers zero EN-DC failure rate by avoiding unnecessary mmWave cell searches when the UE is in NLoS condition. Similarly, when compared with the state-of-the-art AI-based mmWave cell discovery through sparse data only, AISMO enables 3x more EN-DC activations leading to proportionally higher use of mmWave band.**

***Index Terms*—mmWave, Cell Discovery, Artificial Intelligence, Data Sparsity, Emerging Mobile Networks.**

I. Introduction

Recent studies project that global mobile data traffic will increase from 50 Exa Bytes per month to almost 230 Exa Bytes per month in 2026 [1]. This prodigious growth in mobile traffic gives rise to extreme congestion in the high frequency bands deployed by the legacy mobile networks. To cope with this congestion and achieve the sought-after multi-gigabit-per-second wireless connectivity, 5G is relying on new frequency spectrum of 30 GHz to 300 GHz, commonly known as the mmWave spectrum [2]. Recently, sub-6GHz macro base stations (BSs) and mmwave BSs are deployed in conjunction. Recently, sub-6GHz macro base stations (BSs) and mmwave BSs are deployed in conjunction. Macro BS refer to the traditional sub-6 GHz cells. Compared to mmWave cells with smaller footprint, macro BS with higher power cover a larger coverage area. Therefore, sub-6GHz macro BS serve as the coverage layer and the mmWave BS serve as the capacity layer. This is a practical solution because macro BSs are already widely deployed and mmWave BSs alone cannot provide reliable coverage in vast area unless deployed with extremely high density.

The wide-band mmWave BSs while dramatically scales up the system capacity, come with a new challenge with regards to the cell discovery for the User Equipments (UEs). Unlike sub-6GHz cells, mmWave band has much higher frequency, and consequently a higher free space pathloss, higher absorption and low diffraction. Therefore, users in mmWave band experience a much higher overall pathloss and signal attenuation (resulting in beams with Non-Line-of-Sight (NLoS) scenario not being decoded at the UE terminal) in the mmWave band as compared to sub-6GHz (HF), where the cells radiate signal across comparatively bigger area. The high penetration losses, and directivity in mmWave propagation limit its coverage to be a few tens of meters around mmWave BS. To compensate for the higher pathloss in mmWave, more directional antennas and beamforming has to be used to extend the communication range of mmWave cells. However, under these circumstances, UE and BS do not know the directions to transmit (receive) during the initial access phase, thus causing cell discovery issue. This cell discovery issue is addressed in this paper.

A. Related Work and Motivation

Given that cell discovery is a well-known bottleneck in adaptation of mmWave cells at scale, in recent years, researchers have worked on devising suitable strategies to achieve an efficient cell discovery process in mmWave systems, that reduce latency and overhead [3]–[17].

Authors in [16] propose a hybrid beamforming scheme for THz frequency to overcome propagation attenuations and improve the cell coverage. Similarly, authors in [17] develop an iterative channel estimation algorithm for mmWave MIMO

Authorized licensed use limited to: University of Oklahoma Libraries. Downloaded on August 07,2023 at 17:17:36 UTC from IEEE Xplore. Restrictions apply.
© 2023 IEEE. Personal use is permitted, but republication/redistribution requires IEEE permission. See https://www.ieee.org/publications/rights/index.html for more information.

This article has been accepted for publication in IEEE Transactions on Vehicular Technology. This is the author's version which has not been fully edited and content may change prior to final publication. Citation information: DOI 10.1109/TVT.2023.3289718

Table I: Comparison of mmWave cell discovery approaches.

Cell Discovery Method	Reference	Short Description	Pros	Cons
Angle of Arrival Based Method	[3], [4]	UE location estimation based on angle of arrival.	Less overhead and complexity required.	UE requires additional sensors for orientation estimation.
Exhaustive Search Method	[5], [6]	A simple strategy for cell discovery based on sweeping through all possible antenna configurations looking for a rendezvous between BS and UE via brute force.	a. Support for standalone mmWave cell camping. b. Equal chances among all UEs to get network access.	a. Prove ineffective for mobile UEs. b. Low efficiency due to high i. BS energy consumption. ii. UE latency in network access.
Hierarchy/Binary Search Method	[7], [8]	Extension of Exhaustive Search Method where every iteration successively divides the target UE search area by configuring smaller beams.	a. Support for standalone mmWave cell camping. b. Larger probability of UE network access.	a. Too much BS resources spent for each UE. b. Not suitable for area with large number of UEs.
Hybrid Cell Discovery	[9], [10]	UE estimated location is found through exhaustive search, and then hierarchy method refines the beam alignment.	Lower latency than the above two methods.	Not suitable for area with large number of UEs.
Context Based Cell Search	[11], [12]	Search is focused towards the crowded areas known through e.g., call detail record data.	Achieves higher network efficiency, and adaptability to temporal shifting of crowded areas.	a. Low Fairness towards the UEs located in sparsely populated areas. b. Mobile UEs may not be prioritised for search.
Joint Search Method	[13]–[15]	Macro BS sharing the UE location to mmWave BS.	Less mmWave BS resources spent on UE discovery, and lowest latency due to high hit-rate.[a]	a. Configurational complexity due to UE dual connectivity towards macro and mmWave BSs. b. Susceptible to incorrect UE location due to GPS error/indoor location.

[a]hit-rate - Percentage of successful mmWave cell search.

systems. However, the mmWave cell discovery issue is not studied.

In [3], authors utilize the angle of arrival at the BS for UE localization. Authors in [4] fuses the angular information with a map of the environment to provide mmWave BS location. Studies in [3], [4] can help fine tune the mmWave cell transmission direction towards the UE location, however, the initial UE transmission direction towards the mmWave cell, essential for cell discovery still remains an open challenge.

Authors in [5] exploited exhaustive search method and proposed an optimal beamwidth design taking into account the trade-off between mmWave cell search delay and beamforming gain. Meanwhile, authors in [6] introduced the concept of beam discovery signal to help identify the beam used during the exhaustive search method. The comparison of exhaustive search method and hierarchical search method is presented in [7]. The authors concluded that hierarchical search can achieve similar beam alignment performance vis-a-vis exhaustive search with lower overhead. Meanwhile, a hybrid method combining the strengths of the exhaustive and hierarchical method is proposed in [9] that outperforms hierarchical search method in terms of miss-rate (percentage of misdetection), and exhaustive search in terms of discovery delay. Authors in [12] discussed the context based cell search approach where intelligent mmWave BSs steers its beams through a known populated area for UE discovery. Unlike other approaches, this scheme increases hit-rate by avoiding beam transmission towards sparsely populated areas, or towards blockages like trees, buildings, rivers, etc. However, the study in [12] did not discuss the mechanism to cope with NLoS conditions.

Another promising cell discovery approach has been proposed in [13]–[15] where joint collaboration between macro BS and mmWave BS efficiently discovers the UE with the macro BS feeding the UE location to the mmWave BS. Authors in [13] propose macro cell to be in charge of the control plane, and with the increase in demand of data-rate, instruct the nearby mmWave cell to broadcast synchronization signal towards the respective UE location. Athul Prasad et al. [15] analyzed the energy efficiency metric when joint search based mmWave search method is employed for mmWave cell search procedure. Their study exhibited 45% savings in terms of UE power consumption.

While most of the research papers address the mmWave alignment issue between UE and BS, and the analytical model for coverage probability [5], [14], none of the proposed schemes in literature [5]–[17] incorporates NLoS induced coverage hole in the cell search procedure. This is critical due to the extremely sensitive nature of mmWave to blockages as UEs under NLoS condition might render the BS efforts taken towards mmWave cell search procedure totally useless.

Comparison of the relevant works in Table I shows that the efficacy of methods such as exhaustive search, hierarchy/binary search, and hybrid cell discovery is undermined by the increase in the number of UEs in the network. These methods tend to become inefficient as the number of users in the cell increase. While more efficient compared to the three aforementioned approaches, context based cell search lacks the fairness towards the UEs specially the ones located in sparsely populated areas. Moreover, methods that determine UE location based on mmWave cell only also incur high latency and high energy consumption both on the UE and the BS side. Mobility of the UE will further degrade the accuracy of UE location identification using such method. Therefore, unlike the 3GPP-standardized macro base station-based UE

Authorized licensed use limited to: University of Oklahoma Libraries. Downloaded on August 07,2023 at 17:17:36 UTC from IEEE Xplore. Restrictions apply.
© 2023 IEEE. Personal use is permitted, but republication/redistribution requires IEEE permission. See https://www.ieee.org/publications/rights/index.html for more information.

This article has been accepted for publication in IEEE Transactions on Vehicular Technology. This is the author's version which has not been fully edited and content may change prior to final publication. Citation information: DOI 10.1109/TVT.2023.3289718

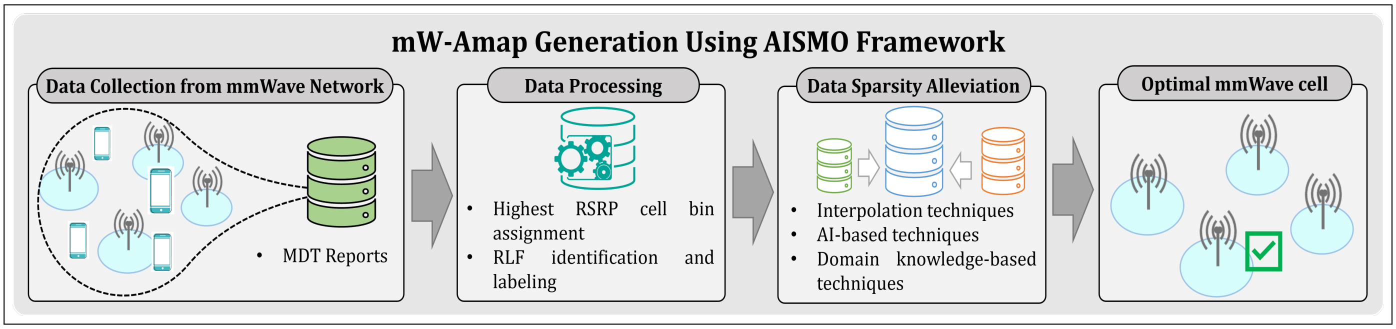

Figure 1: High level overview of mW-Amap generation using sAISMO framework.

Table II: Table of Acronyms

Acronym	Description
LoS	Line-of-Sight
NLoS	Non-Line-of-Sight
RLF	Radio Link Failure
AISMO	AI-enabled Sparse data based MmWave cell discOvery and EN-DC activation framework
MDT	Minimization of Drive Test
mW-MDT	Historic mmWave MDT data having UE GPS location, mmWave cell ID, and RLF indication
EN-DC	E-UTRAN New Radio – Dual Connectivity
NeN	Nearest Neighbor
IDW	Inverse Distance Weighted
NNC	Nearest Neighbor count: **Proposed scheme for enriching sparse mW-MDT data**
WNNC	Weighted Nearest Neighbor count: Another **proposed scheme for enriching sparse mW-MDT data**
SC	Sparsity Scenario
DL	Deep Learning
DNN	Deep Neural Network
mW-map	mmWave map created by cell association i.e. the area of interest is divided into bins. Cell ID of mmWave cell with highest received signal strength is assigned to that bin, as long as the bin is within distance κ from mmWave BS, has LoS with it, and has received signal strength above receiver sensitivity
mW-Smap	mmWave coverage map created by the raw sparse mW-MDT
mW-Amap	mmWave augmented map created by enriching the raw sparse mW-MDT data through, interpolation, NNC, WNNC, or AI: **proposed solution for mmWave cell discovery**
NN-ENDC	Nearest neighbor based mmWave ENDC activation: A state-of-the-art method for benchmarking the proposed solution
Smap-ENDC	mW-Smap based mmWave ENDC activation: A state-of-the-art method for benchmarking the proposed solution
Amap-ENDC	Augmented mW-map based ENDC activation: **proposed solution for ENDC activation for mobile users**

positioning that is already proven to work in practice, real world application of mmWave cell-based UE positioning still needs to be determined.

Given these limitations, in this paper, we propose a NLoS aware cell discovery scheme that builds on the joint search method for cell discovery approach, hereafter referred to as AI-enabled Sparse data based MmWave cell discOvery and EN-DC activation framework (AISMO). In joint search method, macro BS shares the UE location with mmWave BS using high speed Xn interface standardized by 3GPP. By doing so, joint search method reduces the resources spent by the mmWave BS on UE discovery and at the same time offers a high hit-rate which ultimately minimizes the overall latency. As Xn interface is usually optical fiber based or have higher capacity, the effect of small amount of additional signaling needed for AISMO is expected to be negligible. Fig. 1 shows the high level overview of the AISMO framework used to generate mmWave map having optimal mmWave cell id. Each module in the Fig. 1 has been briefly described below:

1) Log the MDT reports from mmWave cells. MDT data, already standardized by 3GPP, can be retrieved directly from the network [18], [19]. The UE can be set with MDT report logging that includes GPS location, serving signal ID, serving signal strength, and RLF instances.
2) Process the collected data from item #1 to create cell ID based mmWave cell association maps, here after referred to as mW-maps. mW-map is generated using the cell ID of mmWave cell with highest received signal strength observed in that bin, as long as the bin is within the maximum allowable distance from mmWave BS, has LoS based signal reception, and has received signal strength above receiver sensitivity. mW-map also contain Radio Link Failures (RLFs) and coverage hole information.
3) Due to sparsity in the MDT data, the generated mW-maps are also expected to be sparse (mW-Smaps). Apply interpolation, domain knowledge, or Artificial Intelligence (AI) based enrichment techniques to address the MDT data sparsity and complete the mW-Smaps transforming them into augmented mW-maps, hereafter referred to as mW-Amaps.
4) Use the generated mW-Amaps to identify the optimal mmWave cell (nearest cell with clear LoS). Using mW-Amaps, AISMO prevents cell association attempt for UEs under incomplete LoS (or NLoS), thereby preventing unnecessary mmWave cell discovery searches.

The terminology and acronyms used in this paper are defined in Table II.

B. Contribution

The main contributions of this paper can be summarized as follows:

- To the best of the authors' knowledge, this is the first paper to present a joint search based mmWave NLoS aware cell discovery framework built using realistic sparse mmWave MDT data consisting of RLFs, coverage holes, and serving mmWave cell identifiers.

Authorized licensed use limited to: University of Oklahoma Libraries. Downloaded on August 07,2023 at 17:17:36 UTC from IEEE Xplore. Restrictions apply.
© 2023 IEEE. Personal use is permitted, but republication/redistribution requires IEEE permission. See https://www.ieee.org/publications/rights/index.html for more information.

This article has been accepted for publication in IEEE Transactions on Vehicular Technology. This is the author's version which has not been fully edited and content may change prior to final publication. Citation information: DOI 10.1109/TVT.2023.3289718

- We propose and evaluate several data sparsity coping techniques to predict the optimal mmWave cell in locations from where no prior MDT data are reported. Thus, this is first joint mmWave cell discovery scheme that works with realistically sparse MDT data where only 5-30% of the bins have prior mmWave cell user history.
- A key output of the proposed AISMO framework is the mW-Amaps that contain the cell ID of the optimal mmWave cells for each bin. The mW-Amaps then assist the macro BS to identify optimal mmWave cell for a given UE location.
- We demonstrate through a realistic case study how AISMO can facilitate intelligent activation of E-UTRAN New-Radio Dual Connectivity (EN-DC) [20]. We compare the EN-DC activation rate enabled by AISMO to two state-of-the-art EN-DC activation schemes; a) mmWave cell discovery based on nearest mmWave cell, and b) mmWave cell discovery based on the sparse mmWave MDT data (without data augmentation as leveraged in AISMO).

The rest of the paper is organized as follows. In section II we discuss the data collection of MDT style traces from a realistic mmWave cell deployment scenario. In Section III, we present the state-of-the-art and propose different approaches to augment the sparse mmWave MDT data. Using augmented data, we create mW-Amaps that in turn enable identification of the best mmWave to serve a UE in a given location. We also investigate the tradeoff between the accuracy and computational cost of the most promising mmWave MDT data augmentation techniques. In Section IV we present a case study to evaluate the potential of AISMO for EN-DC activation for 5G mmWave network and benchmark its performance with two state-of-the-art techniques. We conclude the paper in Section V.

II. Data Collection From a Realistic mmWave Environment

In this study we use synthetic data because of the challenges associated with real data collection and analytical modeling as explained in following subsections.

A. Challenges in mmWave Data Collection from Real Network

Collecting mmWave MDT data from a live network though possible in theory, is impractical because of several reasons. First, mmWave networks are not widely deployed in most location. Even for select deployment areas like Los Angeles, California where some network operators have already deployed mmWave network, data acquisition are difficult and does not constitute a viable campaign as the number of mmWave enabled UEs are scarce. Additionally, existing techniques of mmWave cell discovery are based on exhaustive search and the associated inefficiency in cell discovery contributes to low UEs camping on mmWave cell. This further adds to the difficulty of collecting enough data samples to be deemed useful. Subscriber data confidentiality further hinders data collection from the existing mmWave UEs. Although other means of data collection such as drive test exist, performing this in a congested place like Los Angeles is expensive both in terms of time and resources. Besides, drive test based data collection when compared to MDT style data collection, can provide only traces from paved locations which represent even smaller fraction of the total area of interest.

B. Challenges in Analytical Modeling

For a complex heterogeneous cellular system with realistic mobility, it is extremely challenging to develop a comprehensive and tractable analytical model. Mobility details like handover process combined with intricate inter-dependencies between dynamic heterogeneous network parameters, nonlinear relationships, and various factors such as blockages, terrain, user behavior, interference, and complex antenna patterns further complicate the analytical modeling process. The closest analytical modelling approach for the system considered in this work are the stochastic geometry-based works in [8], [9], [21]–[26] and the works in [27]–[30]. However, these works do not cover realistic user mobility (based on for example historical mobility patterns), 3GPP based intra-frequency handover, inter-frequency handover evaluation criteria, flexibility to configure each base station (transmission power, height, tilt, etc.), dual connectivity (carrier aggregation, EN-DC, NR-NR dual connectivity), and blockage modeling (pre-determined locations and dimensions of blockage, etc.). A tractable analytical model will only be possible if the system is assumed to be a static system, devoid of realistic mobility and by employing numerous simplifications to model its intricate complexities. Relying solely on such an assumption based analytical model would lead to inaccurate predictions and sub-optimal solutions.

C. Synthetic Data Collection through SyntheticNET Upgrade

In the backdrop of the aforementioned challenges, and motivated by successful use of synthetic data for training AI in many fields [31]–[34], in this paper we resort to synthetic data. All the RLF samples used for the simulation are obtained artificially from the simulator. For that, we exploit a 3GPP-compliant state-of-the-art system level simulator named SyntheticNET [35]. SyntheticNET simulator has been calibrated against real network measurements to ensure the validity of the data generated through it. Moreover, SyntheticNET simulator triggers RLF as per 3GPP criteria [20], i.e., when a) UE goes out of sync, b) maximum number of RACH attempts have been reached, or c) when retransmission attempts reach the configured threshold. However, although SyntheticNET, in its current form, supports features related to cell discovery such as 3GPP-based initial cell selection [36], it is tailored more to mimic a network operating on lower frequency bands (i.e., maximum 3.5GHz). To address this issue, we incorporate several upgrades to make SyntheticNET more suitable for mmWave simulation environment.

To model the macroscopic propagation effects in a mmWave simulation environment, first, we utilize a real antenna pattern from a mmWave antenna available commercially [37]. The use of a realistic antenna pattern helps in a more accurate mmWave based coverage modeling. Moreover, instead of using two separate pathloss models for LoS and NLoS scenarios respectively, we utilize a single pathloss model for LoS scenario. For NLoS situations, we model the attenuation caused by

Authorized licensed use limited to: University of Oklahoma Libraries. Downloaded on August 07,2023 at 17:17:36 UTC from IEEE Xplore. Restrictions apply.
© 2023 IEEE. Personal use is permitted, but republication/redistribution requires IEEE permission. See https://www.ieee.org/publications/rights/index.html for more information.

This article has been accepted for publication in IEEE Transactions on Vehicular Technology. This is the author's version which has not been fully edited and content may change prior to final publication. Citation information: DOI 10.1109/TVT.2023.3289718

Table III: Description of Simulation Parameters

Parameter Description	Value
Simulation area	25 km^2
Number of macro BSs	3
Macro cell frequency	2.1 GHz
Number of mmWave BSs	5
mmWave cell frequency	28 GHz
mmWave cell height	10 m
mmWave Transmission Power	20 dBm
Pathloss Exponent	5
Shadowing Standard Deviation	8
Number of UEs per km^2 per Sparsity Scenario (SC)	SC1: 30, SC2: 60, SC3: 120, SC4: 240, SC5: 190
% of Mobile UEs	70%
Mobile UE velocity	60 km/h
Cell range (κ)	1500m
Total Simulation Time	15000 ms

blockage by incorporating actual obstructions in the simulator. This approach is more realistic and practical as the location, dimensions, and even signal degradation respective to each unique obstruction can be accurately configured compared to empirical or analytical pathloss models.

The downlink signal strength R_u^s from the serving mmWave cell s to user u is given by:

$$R_u^s = P_t^s G_u G_u^s \delta_u^s \alpha (r_u^s)^{-\beta} \tag{1}$$

where P_t^s is the transmit power of serving mmWave cell s, G_u is the gain of user equipment, G_u^s is the transmitter antenna gain of the mmWave cell s towards user u, δ_u^s is the shadowing observed from the mmWave cell s at the location of user u, α is the pathloss constant, β is the pathloss exponent and r_u^s represent the distance of user u from cell s. The values of α, β, and δ are based from the study conducted in [38].

D. Simulation Setup and Modeling Sparsity

We use an area of size 5km $\times$ 5km for the simulation as shown in Fig. 2(a). The 25km^2 simulation area is further divided into one million 5m $\times$ 5m bins. We deploy a heterogeneous network with three macro BSs radiating at 2.1GHz frequency, and five omni-directional mmWave BSs operating at 28GHz band. Fig. 2(a) also shows the system model diagram of the deployed location of the macro and mmWave cells. Moreover, several obstructions are put in place to realistically model the NLoS scenario. The rest of the system-level simulation parameters are summarized in Table III.

The key idea of the proposed AISMO framework is to leverage historical mmWave MDT data to build coverage maps that can be exploited by macro BS to identify the optimal mmWave cell for a user in a given location. However, given the non-uniform nature of user distribution, a large fraction of the area of interest is expected to have no historical MDT data. Particularly, emerging mobile networks operating on the mmWave bands will initially observe low utilization due to the low number of readily available devices supporting mmWave. As a result, the overall MDT data from a mmWave network is anticipated to be even more sparse.

To model this inherent sparsity in the MDT data, we utilize SyntheticNET and present five sparsity scenarios (SC), each with different user densities. SC1, SC2, SC3, and SC4 represent scenarios wherein 5%, 10%, 20%, and 30% (corresponding to the initial user deployments ranging from 30, 60, 120, and 240 per km^2 with 1500 samples per user for each SC respectively) of the total one million 5m $\times$ 5m bins have available data, respectively, and the remaining bins have no data. These SCs are generated by varying the number of users distributed in the network. The number of UEs per SC is summarized in in Table III. While the aforementioned SCs have uniformly distributed UEs, an additional SC, SC5, represents a more realistic non-uniform distribution of UEs. 70% of the UEs in all the five sparsity scenarios are configured to be mobile following random waypoint mobility model. The fifth SC with non-uniform user distribution represents areas with different user densities as typically, during peak hours, hotspot areas have much higher traffic than neighboring areas.

In all SCs, UEs were deployed according to uniform random distribution, where each UE had an equal probability of going into any bin. At the end of the simulation, 15,000 unique data snapshots were collected from test users. It should be noted that UEs may end up in the same bin during simulation, but because the nearest cell with line-of-sight is used for mmWave cell association, the cell-identifier data in each bin will always be identical.

During the simulation, UEs are configured to camp initially on 2.1GHz macro cells, that provide coverage to UEs within the target area. We assume the macro cells to have accurate UE location information to share with the mmWave cells, thus conforming to the joint search method. Moreover, we assume the exact UE location known to the mmWave cells enables them to achieve perfect beam alignment with the UE. This conforms with the mmWave environment where mmWave cells with beamforming will have pencil-like beams and mmWave UE will have better signal reception than in the case of macro cells. UEs served by the macro cell then attempt mmWave cell camping to the nearest mmWave BS. If the UE fails the mmWave cell camping, it attempts to camp on the second nearest mmWave BS. This process continues until the UE successfully camps to a mmWave cell, fails to find a suitable mmWave cell (for the configured number of attempts), or the distance between the UE and mmWave BS exceeds the cell range denoted by κ. The parameter κ is a common parameter used in the existing mobile networks that prevents far away UEs to camp on an overshooting cell. As a result, UEs can be ensured to have good signal strength and reduced uplink interference from distant UEs. In our simulation, we use a κ value of 1500m to limit the mmWave band small cells' coverage from far away UEs. Note that the beamforming technique can helps mmWave cells to transmit high SINR signal to even UEs located in cell edge.

We record the RLFs of the mobile UEs camped on the mmWave cell as they travel through the designated network area. The RLFs happen due to the drastic signal deterioration from the NLoS reception induced by the blockage between the UE and mmWave BS. Similarly, out of coverage scenario will be observed due to UE getting farther from the serving mmWave BS by a distance greater than κ. Furthermore, the failed mmWave cell camping attempts due to the absence of an

Authorized licensed use limited to: University of Oklahoma Libraries. Downloaded on August 07,2023 at 17:17:36 UTC from IEEE Xplore. Restrictions apply.
© 2023 IEEE. Personal use is permitted, but republication/redistribution requires IEEE permission. See https://www.ieee.org/publications/rights/index.html for more information.

This article has been accepted for publication in IEEE Transactions on Vehicular Technology. This is the author's version which has not been fully edited and
content may change prior to final publication. Citation information: DOI 10.1109/TVT.2023.3289718

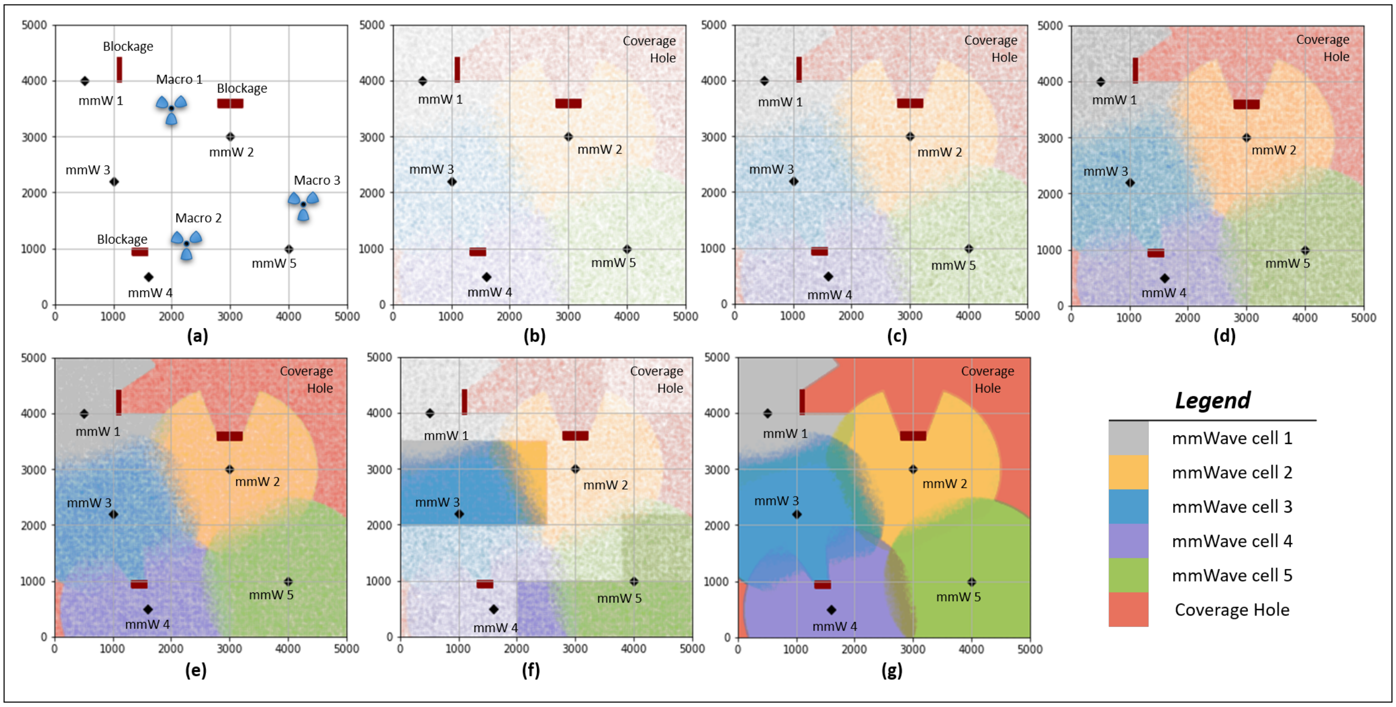

Figure 2: (a) System model with macro cell, mmWave cell and blockage locations. mW-map for (b) SC1 - 5% uniform sparse data, (c) SC2 - 10% uniform sparse data, (d) SC3 - uniform sparse 20% data, (e) SC4 - uniform sparse 30% data, (f) SC5 - non-uniform sparse data, and (g) Ground truth.

optimal mmWave cell for the static and mobile UEs are also recorded. Both the RLF and failed cell camping are marked as coverage holes in this work. Fig. 2(b-f) illustrates the different sparsity levels in SC1 to SC5, the resultant coverage hole and suitable mmWave cell ID map obtained from the simulation results. Fig. 2(b-f) also represent the mmWave cell ID simulated where UEs camped on and identify coverage holes in red color. Finally, we increase the number of UEs to 2000 and uniformly disperse the UEs before running the simulation. The data gathered through this setup are not sparse and serves as the ground truth (Fig. 2(g)) to verify our results presented in the next section.

Location and size of obstacles is crucial in determining the LoS or NLoS conditions, However, we omit this explicit information as an input to the AI model as this information would require a comprehensive and continual survey of the area. Such a survey is a costly, time-consuming, and resource-intensive task given the number of mmWave cells that are expected to be deployed in the near future. To address this issue, our AI model is trained using actual cell identifier (PCI) and RLF data already present in MDT data. The AI model implicitly learns the impact obstacles from the occurrence of RLF. This smart mechanism to learn the impact of obstacles from MDT data indirectly, without requiring direct survey-based knowledge of location and height of obstacles is one of the core contributions of the paper. Based on this learning, model does not make any optimal mmWave cell prediction for the obstructed areas. Additionally, by periodically retraining the AI model with new MDT data, any changes in the size or location of the obstacles can be accounted for in the new AI model.

III. Identifying Optimal mmWave Cell

In this section, we discuss our proposed solution to identify the optimal mmWave cell for each UE. However, a major challenge in this identification is data sparsity. Addressing data sparsity is essential to predict the optimal mmWave cell specially in areas where no prior information of mmWave cell camping due to no UE information is available. Using the joint search method, a macro cell serving a mmWave compatible UE can share the UE location to the known optimal mmWave cell for efficient and effective mmWave cell camping. The data sparsity mitigation techniques we investigate, evaluate and compare for optimal mmWave cell identification include interpolation techniques, domain knowledge-based custom algorithms, and artificial intelligence (AI)-based algorithms.

In the initial phase, we can achieve cell discovery using any of the state-of-the-art approach mentioned in Table I. The sparse data obtained through the state-of-the-art cell discovery approach can be then augmented by the sparsity alleviation technique discussed and analyzed in this paper to create mW-Amap. Later on, we can periodically update the mW-Amap using the MDT obtained on the network operated by AISMO. This continual update is important to cater for any environmental or structural change in the mmWave cell coverage area.

A. Leveraging Interpolation Techniques for Optimal mmWave Cell Identification

Recent studies have shown the potential of different spatial interpolation techniques to address the MDT data sparsity challenge in cellular networks [31]. In this paper, we leverage interpolation techniques that have been shown to work well

Authorized licensed use limited to: University of Oklahoma Libraries. Downloaded on August 07,2023 at 17:17:36 UTC from IEEE Xplore. Restrictions apply.
© 2023 IEEE. Personal use is permitted, but republication/redistribution requires IEEE permission. See https://www.ieee.org/publications/rights/index.html for more information.

This article has been accepted for publication in IEEE Transactions on Vehicular Technology. This is the author's version which has not been fully edited and content may change prior to final publication. Citation information: DOI 10.1109/TVT.2023.3289718

in [31] including moving average, inverse distance weighted, and nearest neighbor. A brief description of each technique is given below:

- Nearest Neighbor - The NeN method, also known as proximal interpolation or point sampling, estimates the unknown bin value by calculating the Euclidean distances between that bin and the locations of the known bin measurements and then selecting the measurement with the minimum Euclidean distance. Although the nearest neighbor approach has low complexity, it can result in sharp transitions between adjacent bin values and can also increase noise, especially at the boundary of different cell zones [39].
- Inverse Distance Weighted (IDW) - Assuming that the data are strongly correlated in space, the classical IDW method estimates the value of the unlabeled bins by calculating a weighted arithmetic average of the neighboring known bin values. Each known value is weighted with a weight that is equal to the inverse of the distance between the location of the missing value and the location of the known value raised to a power, p. An advantage of IDW method is the ease of implementation since it is intuitive. This interpolation works best with evenly distributed data points. However, in the case of non-uniform distribution of measurements or unevenly distributed data clusters, it is sensitive to measurement outliers and introduces significant errors. It also becomes less accurate in case of discrete data as the weighted arithmetic average in that case needs to be rounded off to a discrete value. Moreover, its computational complexity increases as the number of observed spatial points increases, leading to inefficiency of this method when the number of data points are large.
- Moving Average - The value of the unlabeled bin in this case equals the arithmetic average of the known neighboring bin data. Mathematically, for moving average method is same as IDW with power $p = 0$.

These interpolation techniques work best specially in cases where the available sparse data are somewhat representative of the whole data or exhibits some degree of spatial correlation [31]. However, in situations where the available data are sparse or non-representative, these methods are likely to perform poorly. Therefore, for those scenarios, alternative methods must be investigated for the problem of interest.

B. Domain Knowledge Based Custom Algorithms for Optimal mmWave Cell Identification

To overcome the aforementioned shortcomings of interpolation-based methods to cope with mmWave MDT data sparsity, in this subsection we present two domain knowledge-based algorithms to address the data sparsity. A range of sparsity addressing techniques have been proposed and analyzed in our earlier work [40]–[42] for completing coverage maps [31]. To the best of the authors' knowledge, this is the first study to analyze a domain knowledge-based sparsity alleviation method in the form of NNC and WNNC for enhancing mW-map. However, NNC is not a novel idea as it is similar to commonly used imputation using a) mean and b) mode sparsity alleviation techniques. On their other hand WNNC uses weighted nearest neighbor information. Thus, WNNC is an advanced form of K-Nearest Neighbor (KNN), where it uses domain knowledge aware (tier control and GPS accuracy per area) weighting metric to the spatial data for supplementing the sparse data.

Algorithm 1: Weighted Nearest Neighbors Count (WNNC)

```
Initialize K, GPSaccuracy, BINsize, and Label ;
  // Label: vector of mmW PCIs with 0
  representing coverage hole
for Every bin b do
    if b is unlabeled then
        Initialize Cweight ;      // Cweight: vector
         representing cumulative weight against
         each entry of Label vector
        for tier k = 1 to K do
            fetch bins_k from tier k compute weight w_k
             for index i = 1 to size(Label) do
                CUMweight[i] += w_k ×
                 count(Label[i] in bins_k)
            end
        end
        if max(CUMweight) > 0 then
            label b with PCI having maximum
             CUMweight
        else
            Do Nothing;        // Not enough data.
             Surrounding bins are empty
        end
    else
        Do nothing;
    end
end
```

- Nearest Neighbor Count (NNC): NNC fills up the unlabeled bin using the values of the labeled bin with the maximum number of occurrences in the surrounding tiers represented as K. Unlike legacy interpolation method, this domain aware method does not introduce rounding off error. NNC, when used with large number of tiers (K), tends to complete more empty bins. This property is particularly useful for areas with ultra-sparse populations. However, using large values of K might not be favorable under the mmWave environment. High LoS dependency of mmWave frequencies may tend to mislabel the empty bins where the UEs cannot be serviced by the mislabeled cell due to some narrow blockages. This limitation can aggravate further when using large bin sizes.
- Weighted Nearest Neighbor Count (WNNC): WNNC addresses the aforementioned drawback of NNC by applying a unique weight w to each tier around the unlabeled bin. The weight w decreases gradually as we move away from the unlabeled data to the outer tier. The weight w_k assigned to a tier $k \in [1, K]$ can be represented mathematically as:

Authorized licensed use limited to: University of Oklahoma Libraries. Downloaded on August 07,2023 at 17:17:36 UTC from IEEE Xplore. Restrictions apply.
© 2023 IEEE. Personal use is permitted, but republication/redistribution requires IEEE permission. See https://www.ieee.org/publications/rights/index.html for more information.

This article has been accepted for publication in IEEE Transactions on Vehicular Technology. This is the author's version which has not been fully edited and content may change prior to final publication. Citation information: DOI 10.1109/TVT.2023.3289718

Table IV: Deep learning hyper-parameters for optimal mmWave cell identifier model.

Hyper-parameter Name	Search Range/Value
DNN Depth d	$\{1,2,3,4,5,6\}$
DNN Width w	$\{5,8,10,12,16\}$
Activation Function (Hidden Layers)	Relu
Activation Function (Output Layers)	Sigmoid
Optimizer	Adam (Gradient Descent)
Loss Metric	Binary Cross Entropy

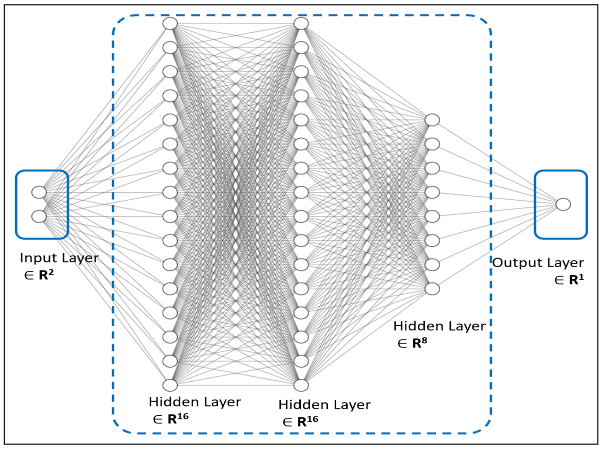

Figure 3: Structure of the deep learning based model for predicting optimal mmWave cell for a given UE location.

$$w_k = \frac{\psi}{k \times \omega} \tag{2}$$

where ψ represents GPS accuracy in meters and the bin size is denoted by ω (also in metres). Details about the operation of WNNC is shown in algorithm 1. While in the simulation setup (Fig. 2) we assume that the macro BS does not contribute to the UE positioning error i.e. GPS, the GPS positioning error has been incorporated as a component in the weight metric to allow for the GPS based positioning error [43]. To compensate for the importance of LoS in mmWave transmission in places with high GPS accuracy, more weight is given to the nearest bins (lowest tier). In contrast, bins further away (higher tier) receive less weight because they contribute less to filling empty bins.

C. Artificial Intelligence Assisted Optimal mmWave Cell Identification

Wireless cellular networks are highly dynamic systems where traffic intensity, and user mobility patterns are continuously changing after few intervals. We therefore created several machine learning models to compare the training time and accuracy with the methods discussed in earlier subsections. In this subsection we describe machine learning algorithms that we leverage to alleviate sparsity issue and construct a mW-map representing the optimal mmWave cells for the UEs. The available sparse data are scaled and used to train and test several AI techniques for creating a best-performing model for determining optimal mmWave cell as a function of UE location. We begin by splitting the sparse data into a training and a test dataset. We investigate the performance of state-of-the-art AI algorithms for filling in the missing values in the sparse data based mmWave maps. These include Naïve Bayes, KNN, decision trees, SVM, and deep learning based models. We optimize the performance of each these algorithms through intensive hyper parameter tuning.

Table V: Time to build mW-Amap.

Use Case	Labeled Bins	Unlabeled Bins	Time to Build mW-Amap. Nearest Neighbor	WNNC (K=10)	DL
SC1	50,000	950,000	6.4sec	21.2Hrs	12mins
SC2	100,000	900,000	6.9sec	20.9Hrs	45mins
SC3	200,000	800,000	7.7sec	19.4Hrs	43mins
SC4	300,000	700,000	8.7sec	18.7Hrs	48mins
SC5	187,176	812,824	7.4sec	19.5Hrs	57mins

Deep neural network-based model are particularly prone to over fitting or under fitting given the large degrees of freedom. To avoid under-fitting or over-fitting, we investigate a variety of DNN architectures with a range of hyper-parameters as shown in Table IV. Our investigation shows that a DNN model with fully connected three hidden layers having 16, 16, and 8 neurons respectively, (shown in Fig. 3) yields the best results. This DNN model is trained using an epoch size of 200 and a batch size of 10.

D. Performance Comparison Between the Different Techniques for Optimal mmWave Cell Identification

We evaluate the potential of the aforementioned approaches to identify the optimal mmWave cell using accuracy as the performance metric. Among the interpolation techniques, NeN outperforms the other two techniques, (i.e., IDW and moving average) with accuracy of more than 90% for all the SCs as shown in Fig. 4(a). However, even the best interpolation technique falls short compared to the proposed domain knowledge-based custom algorithms NNC and WNNC. Fig. 4(b) illustrates the accuracy for all five sparsity scenarios obtained with K of 5, 10, and 20 for both NNC and WNNC. Results show that lower K may fail to predict 100% of the target area as evident with the lack of data when $K = 5$ in more sparse data (i.e., SC1 and SC2). On the contrary, higher K will incorporate more neighboring bins to predict the missing bin at the cost of lower accuracy. K of 10 yields the best accuracy in predicting optimal mmWave cell. Comparison of NNC and WNNC performances reveal WNNC yields better results than NNC with the inclusion of domain knowledge assisted weight metric that gives more weightage to lower-tier neighboring bins. Accuracy of as high as 96% can be achieved when using WNNC.

While WNNC shows promising results in identifying the optimal mmWave cell under sparse conditions, it is computationally expensive as shown in Table V. It takes more than 18 hours to generate a complete mW-map using WNNC for any sparsity scenario. However, the processing time can be reduced by using using commercial grade high performance servers having parallel computing support. Meanwhile although interpolation based method NeN can generate the complete map in just seconds, it yields accuracy much lower than WNNC.

Authorized licensed use limited to: University of Oklahoma Libraries. Downloaded on August 07,2023 at 17:17:36 UTC from IEEE Xplore. Restrictions apply.
© 2023 IEEE. Personal use is permitted, but republication/redistribution requires IEEE permission. See https://www.ieee.org/publications/rights/index.html for more information.

This article has been accepted for publication in IEEE Transactions on Vehicular Technology. This is the author's version which has not been fully edited and content may change prior to final publication. Citation information: DOI 10.1109/TVT.2023.3289718

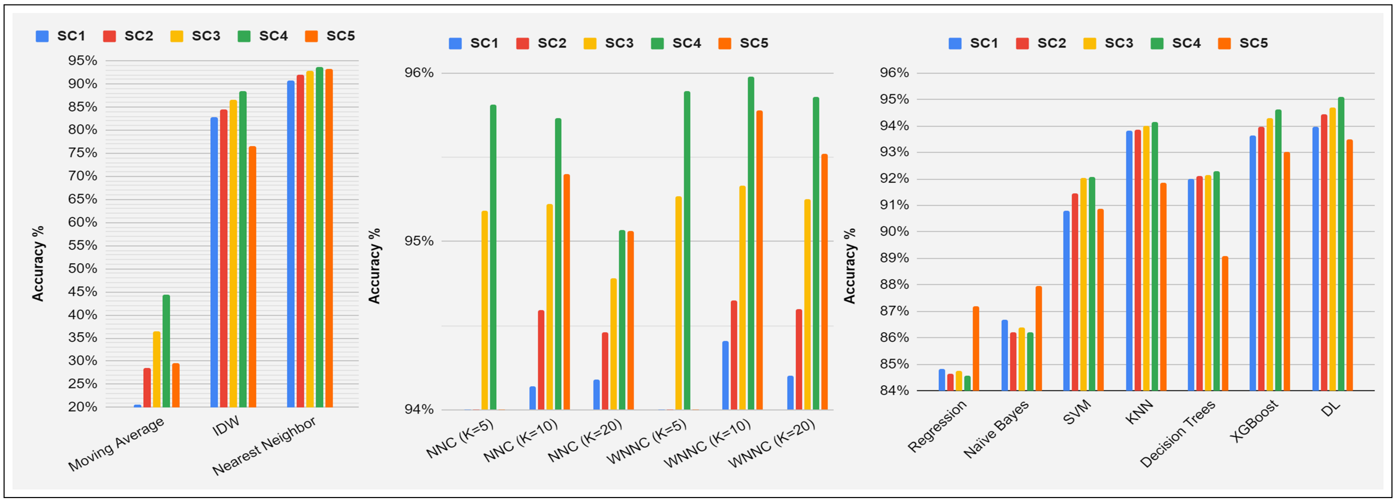

Figure 4: Optimal mmWave cell identification for Sparsity Scenario 1-5 using (a) Traditional Interpolation techniques, (b) Custom Algorithms, (c) Machine Learning.

These limitations of the interpolation-based and custom algorithm-based techniques can be addressed by leveraging AI-based solutions. Fig. 4(c) shows the accuracy of predicting the optimal mmWave cell for various machine learning models trained on the same dataset. Results illustrates the accuracy of optimal cell prediction increase with the increase in available samples (SC1 to SC4). Moreover, results also shows that the DL model gives the best result with an accuracy of almost 95%. Although the accuracy of the DL model is slightly lower compared to the proposed best performing WNNC (96%), the DL model only takes 45 minutes to build mW-Amap as shown in Table V. DL-based models are effective especially for the scenarios where signal reception at different times of the day varies due to different UE mobility and traffic dynamics. As a result, the optimal mmWave cell maps need to be continuously tuned with the dynamically changing conditions mentioned above.

Finally, we provide a visualization of the decision boundary plot for approach that yields the best results in each of the three set of techniques discussed as shown in Fig. 5. This figure validates the higher accuracy generated by the WNNC and DL as manifested by the more prominent boundaries among the mmWave cells compared to interpolation based nearest neighbor technique.

IV. Case Study - EN-DC Activation for mmWave Band

A. Background of EN-DC Activation Problem

The proposed joint search-based mmWave cell discovery solution is well suited for EN-DC activation. As per 3GPP Release 15 specification 37.863 [44], EN-DC allows 5G capable UEs to simultaneously connect to a 4G and 5G BSs. EN-DC activation requires UE to first establish a user-plane and control-plane to a 4G mobile network. Later on, UE searches for an optimal 5G BS and establishes a user plane upon successful discovery of a nearby 5G BS. This non-standalone 5G network deployment helps the mobile operators to reduce the capital expenditure (CAPEX) and thereby accelerating the penetration of 5G networks in developing countries. More details on EN-DC can be found in [20].

The huge resource requirements of bandwidth-hungry applications while keeping in view the over-congested high-frequency bands can be addressed by activating EN-DC using mmWave band of 5G cells. However, EN-DC activation remains as an open problem that requires intelligent solution, particularly in mmWave network. This is because, if user is prompted to attach to sub optimal mmWave cell, it can lead to poorer performance and increased signaling overhead compared to 4G only connectivity, and without reaping much benefits for the user or the network.

The solution to activate EN-DC has to take into account the risk of RLF as analyzed in [20] for 5G/4G network operating on sub-6 GHz frequencies. In [20] the proposed scheme relies on past RLF data on 5G cells to minimize the aforementioned risks. The EN-DC activation problem becomes even more complex if the 5G cell is on mmWave band due to the challenges stemming from mmWave coverage reliability, mmWave cell discovery, and need for the cell beam alignment to the exact UE position. All these conditions must be met for the EN-DC to become successful in mmWave 5G network.

B. Proposed Framework of EN-DC Activation for mmWave Cells

We propose an EN-DC activation solution that leverages the mW-maps constructed through the sparse mmWave MDT data using the approaches presented in the last section. The historical data from UE traces collected from both the 5G standalone, and EN-DC activated UEs contains the serving mmWave cell information against the UE location. The UE traces also contains the RLF data observed due to either NLoS induced signal deterioration or due to a high pathloss situation (where UE and BS distance exceeds cell range κ). The approaches mentioned in Section III can be applied to this mmWave MDT data collected from the network to create the mW-maps and then identify the optimal 5G mmWave cell for a UE based on its reported location. This can help not only in 5G mmWave cell discovery but assist in mmWave cell

Authorized licensed use limited to: University of Oklahoma Libraries. Downloaded on August 07,2023 at 17:17:36 UTC from IEEE Xplore. Restrictions apply.
© 2023 IEEE. Personal use is permitted, but republication/redistribution requires IEEE permission. See https://www.ieee.org/publications/rights/index.html for more information.

This article has been accepted for publication in IEEE Transactions on Vehicular Technology. This is the author's version which has not been fully edited and content may change prior to final publication. Citation information: DOI 10.1109/TVT.2023.3289718

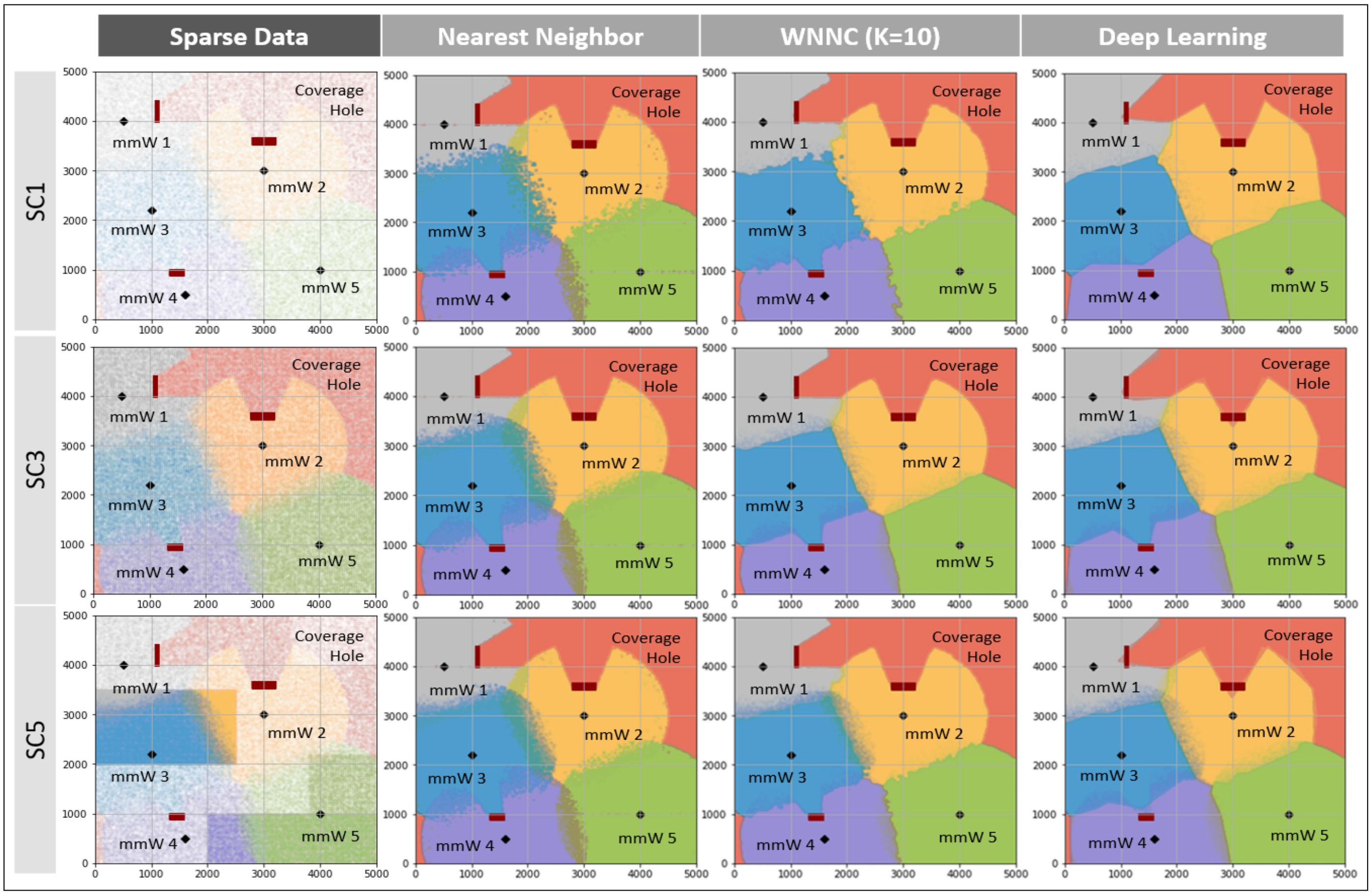

Figure 5: Optimal mmWave cell map predicted using Nearest Neighbor, WNNC (K=10), and DL.

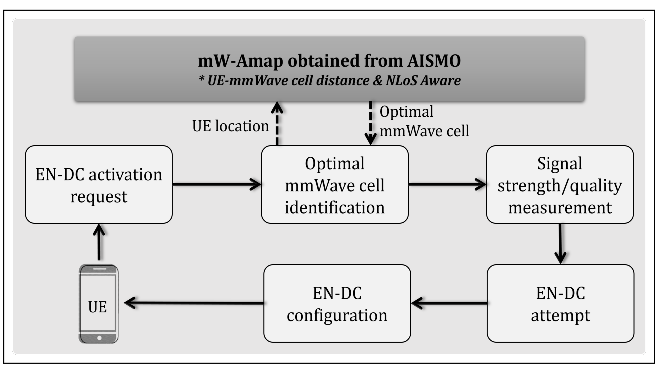

Figure 6: EN-DC activation to optimal mmWave cell using mW-Amap generated by AISMO framework.

beam alignment required to maintain reliable communication for mobile UEs. Fig. 6, presents the schematic of the proposed EN-DC activation scheme. The fact that the proposed scheme is centralized, and the optimal mmWave cell is chosen from the centrally constructed mW-maps, as the one that has the best past performance in terms of received signal strength and low RLF risk makes this scheme superior compared to the state-of-the-art nearest mmWave cell selection.

C. Performance Analysis of the proposed Amap-EN-DC activation solution for mmWave cells

To evaluate the potential of the proposed EN-DC activation scheme, we run a simulation for 300 EN-DC capable UEs, 70% of which move with a constant speed of 60km/h using random waypoint model. The system model used is the same as shown earlier in Fig. 2(a), where 4G macro BSs act as the coverage layer and 5G mmWave cells take the role of the capacity layer to address the needs of bandwidth-hungry applications by activation of EN-DC where applicable. We assume that the UEs already camped on 4G macro cell. When a 5G service is desired, UE requests EN-DC activation. Followed by this request, macro cell initiates mmWave cell discovery using joint search method where the UE's location is shared by the 4G macro cell to the respective optimal 5G mmWave cell. Our proposed method to determine the optimal mmWave cell for EN-DC activation i.e., Amap-ENDC is described in the last subsection and further illustrated in Fig. 6. We benchmark the performance of the proposed Amap-ENDC against following two state-of-the-art EN-DC activation approaches:

- Connecting to the nearest mmWave BS (NN-ENDC) - in this simple approach, 4G macro cell directs the 5G mmWave cell located nearest to the candidate UE to establish the EN-DC connection, without taking into consideration the location of the blockages or quality

Authorized licensed use limited to: University of Oklahoma Libraries. Downloaded on August 07,2023 at 17:17:36 UTC from IEEE Xplore. Restrictions apply.
© 2023 IEEE. Personal use is permitted, but republication/redistribution requires IEEE permission. See https://www.ieee.org/publications/rights/index.html for more information.

This article has been accepted for publication in IEEE Transactions on Vehicular Technology. This is the author's version which has not been fully edited and content may change prior to final publication. Citation information: DOI 10.1109/TVT.2023.3289718

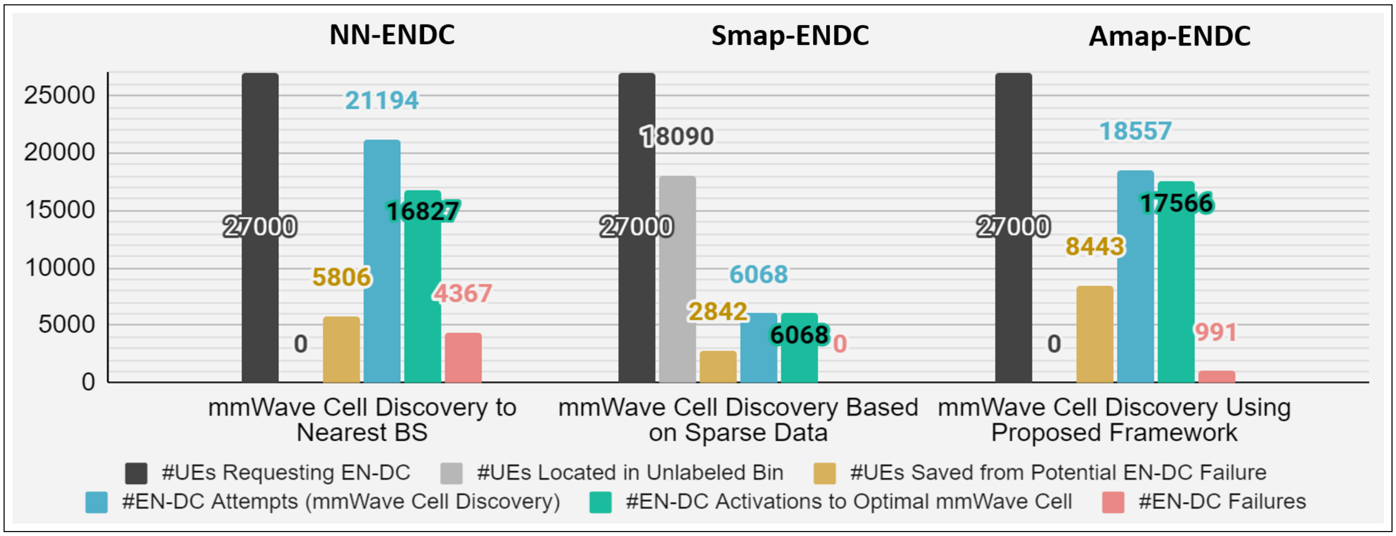

Figure 7: Comparison of EN-DC activation KPIs for 5G mmWave cells.

of coverage observed from past connections with UE from the same location. This approach while being very simple to implement, is prone to failed ENDC attempts as revealed in results section.

- mmWave cell association to best cell from mW-map generated from the sparse mmWave MDT data (Smap-ENDC). In this approach, historical data obtained at the UE location are leveraged to create mW-maps and to identify the optimal mmWave cell. mmWave cell discovery for EN-DC activation terminates if the UE is located in a bin in the mW-map where prior UE traces are not available. Given the sparsity of real MDT data for mmWave cells, this scenario where Smap-ENDC is unable to suggest an optimal mmWave cell is expected to happen quite often leading to lower EN-DC activation rate.

Results in Fig. 7 shows that although NN-ENDC approach triggers a large number of EN-DC attempts (21194), successful EN-DC activations are much less due to around 4367 EN-DC failures. The large number of EN-DC failures is brought by the 4G macro cells being unaware of the blocking locations and the absence of NLoS aware mW-map. Note that EN-DC failure here refers to the UE with failed mmWave cell discovery or due to UE camping to the sub-optimal mmWave cell. On the other hand, the second approach i.e., Smap-ENDC, achieves zero EN-DC failures, but with a very few numbers of EN-DC attempts. This is due to the small fraction of bins in the raw sparse data based mW-maps being labeled. A sparsity of 30% that is realistic representation of user distributions in a typical city is considered in this case (similar as SC4). Fig. 7 shows that 18090 bins are unlabeled and for the UE in any of the unlabeled bins in the mW-map, the macro cell does not proceed with mmWave cell discovery due to the absence of information about the optimal mmWave cell for UEs in those particular bins.

Finally, the best EN-DC KPIs are obtained using the proposed Amap-ENDC scheme. We use DL-assisted augmentation of the MDT data to create the complete mmW-maps from the raw mmWave MDT data as explained in Section III, due to affordable computational complexity and yet second best accuracy. Fig. 7 shows that compared to the other two ENDC activation approaches discussed above, the maximum number of EN-DC activations are observed when attempting mmWave cell discovery using our proposed approach. This is due to the interpolation of the sparse data which allows macro BS to effectively predict the optimal mmWave cell against the UE location. Moreover, macro BS avoid unnecessary mmWave cell search attempts due to the knowledge of the UE being in the coverage hole. The NN-ENDC approach which attempts cell discovery for the nearest mmWave BS has only the knowledge of the number of UEs farther from the mmWave BS than κ. On the contrary, the proposed Amap-ENDC scheme knowing the number of UEs out of the configured cell radius κ, along with the NLoS aware mW-map results in an efficient EN-DC activation with just ∼5% EN-DC failures (991 failures out of 18557 EN-DC attempts).

V. Conclusion

The mmWave cell discovery procedure is an arduous task, due to the highly directional nature of mmWave transmission which is crucial to compensate the severe propagation losses. The joint search method is the most promising cell discovery approach where the high-frequency macro cell aids the mmWave cell discovery by sharing the UE location to the nearby mmWave cell. However, the knowledge of the optimal mmWave cell is crucial to the success of mmWave cell discovery. This is due to the peculiar nature of mmWave cells where signal level deteriorates dramatically when UE goes under NLoS scenario. To address this issue, we propose the AISMO framework, where MDT data can be leveraged to build an mW-map. Since sparsity is typically intrinsic in the mobile network data, we employ data sparsity alleviation techniques to build a comprehensive UE-BS distance aware as well as NLoS aware optimal mmWave cell map called mW-Amap. Results from a mmWave-enabled 3GPP-compliant simulator SyntheticNET show that optimal mmWave cell can

Authorized licensed use limited to: University of Oklahoma Libraries. Downloaded on August 07,2023 at 17:17:36 UTC from IEEE Xplore. Restrictions apply.
© 2023 IEEE. Personal use is permitted, but republication/redistribution requires IEEE permission. See https://www.ieee.org/publications/rights/index.html for more information.

be predicted with accuracy of 96% using a domain knowledge-based custom WNNC algorithm. Since UE mobility and traffic dynamics may affect signal reception in different times of the day, we demonstrate how deep learning can be used to build the mW-Amap with 30x lesser time interval than WNNC algorithm, and with the accuracy of 95%. We also present a case study where the proposed AISMO framework is utilized to efficiently enforce EN-DC transmissions between the EN-DC capable UEs and the participating 4G macro cells and 5G mmWave cells. Simulation results show that for a known UE location, mW-Amap obtained from AISMO framework can help achieve 95% EN-DC activations to ideal mmWave cell.

Acknowledgment

This work is supported by the National Science Foundation under Grant Numbers 1718956 and 1730650 and Qatar National Research Fund (QNRF) under Grant No. NPRP12-S 0311-190302. The statements made herein are solely the responsibility of the authors. For more details about these projects please visit: http://www.ai4networks.com.

References

[1] Ericsson, "Ericsson Mobility Report November 2020," Tech. Rep., 2020. [Online]. Available: https://www.ericsson.com/4adc87/assets/local/mobility-report/documents/2020/november-2020-ericsson-mobility-report.pdf

[2] K. Xiao, W. Li, M. Kadoch, and C. Li, "On the Secrecy Capacity of 5G MmWave Small Cell Networks," *IEEE Wireless Communications*, vol. 25, no. 4, pp. 47–51, 2018.

[3] M. Ruble and Güvenç, "Wireless localization for mmWave networks in urban environments," no. 35, 2018.

[4] O. Kanhere and T. S. Rappaport, "Millimeter Wave Position Location using Multipath Differentiation for 3GPP using Field Measurements," in *GLOBECOM 2020 - 2020 IEEE Global Communications Conference*, 2020, pp. 1–7.

[5] J. Fan, L. Han, X. Luo, Y. Zhang, and J. Joung, "Beamwidth design for beam scanning in millimeter-wave cellular networks," *IEEE Transactions on Vehicular Technology*, vol. 69, no. 1, pp. 1111–1116, 2020.

[6] B. Yin, Y. Chen, Z. Zhang, M. Wang, and S. Sun, "Beam Discovery Signal-Based Beam Selection in Millimeter Wave Heterogeneous Networks," *IEEE Access*, vol. 6, pp. 16 314–16 323, 2018.

[7] C. Liu, M. Li, S. V. Hanly, P. Whiting, and I. B. Collings, "Millimeter-wave small cells: Base station discovery, beam alignment, and system design challenges," *IEEE Wireless Communications*, vol. 25, no. 4, pp. 40–46, 2018.

[8] Y. Yang, H. S. Ghadikolaei, C. Fischione, M. Petrova, and K. W. Sung, "Reducing initial cell-search latency in mmwave networks," in *IEEE INFOCOM 2018 - IEEE Conference on Computer Communications Workshops (INFOCOM WKSHPS)*, 2018, pp. 686–691.

[9] S. Habib, S. A. Hassan, A. A. Nasir, and H. Mehrpouyan, "Millimeter wave cell search for initial access: Analysis, design, and implementation," in *2017 13th International Wireless Communications and Mobile Computing Conference (IWCMC)*, 2017, pp. 922–927.

[10] M. Jasim and N. Ghani, "Fast beam discovery for mmwave cellular networks," in *2017 IEEE 18th Wireless and Microwave Technology Conference (WAMICON)*, 2017, pp. 1–6.

[11] I. Filippini, V. Sciancalepore, F. Devoti, and A. Capone, "Fast Cell Discovery in mm-Wave 5G Networks with Context Information," *IEEE Transactions on Mobile Computing*, vol. 17, no. 7, pp. 1538–1552, 2018.

[12] R. Parada and M. Zorzi, "Cell discovery based on historical user's location in mmWave 5G," in *European Wireless 2017; 23th European Wireless Conference*, 2017, pp. 1–6.

[13] A. S. Marcano and H. L. Christiansen, "Macro Cell Assisted Cell Discovery Method for 5G Mobile Networks," in *2016 IEEE 83rd Vehicular Technology Conference (VTC Spring)*, 2016, pp. 1–5.

[14] C. Sun, J. Zhang, X. Zhang, and W. Wang, "Macro-Assisted Millimeter-Wave Small Cell Discovery in Ultra Dense Wireless Network," in *2017 IEEE International Conference on Internet of Things (iThings) and IEEE Green Computing and Communications (GreenCom) and IEEE Cyber, Physical and Social Computing (CPSCom) and IEEE Smart Data (SmartData)*, 2017, pp. 545–551.

[15] A. Prasad, P. Lunden, K. Valkealahti, M. Moisio, and M. A. Uusitalo, "Network assisted small cell discovery in multi-layer and mmWave networks," in *2015 IEEE Conference on Standards for Communications and Networking (CSCN)*, 2015, pp. 118–123.

[16] C. Huang, Z. Yang, G. C. Alexandropoulos, K. Xiong, L. Wei, C. Yuen, Z. Zhang, and M. Debbah, "Multi-hop ris-empowered terahertz communications: A drl-based hybrid beamforming design," *IEEE Journal on Selected Areas in Communications*, vol. 39, no. 6, pp. 1663–1677, 2021.

[17] C. Huang, L. Liu, C. Yuen, and S. Sun, "Iterative channel estimation using lse and sparse message passing for mmwave mimo systems," *IEEE Transactions on Signal Processing*, vol. 67, no. 1, pp. 245–259, 2019.

[18] 3rd Generation Partnership Project, "Universal Terrestrial Radio Access (UTRA) and Evolved Universal Terrestrial Radio Access (E-UTRA); Radio measurement collection for Minimization of Drive Tests (MDT); Overall description; Stage 2 (Release 10), 3GPP Standard TS 37.320, Version 10.2.0," Tech. Rep., June 2011.

[19] H. N. Qureshi and A. Imran, "Optimal bin width for autonomous coverage estimation using mdt reports in the presence of user positioning error," *IEEE Communications Letters*, vol. 23, no. 4, pp. 716–719, 2019.

[20] S. M. A. Zaidi, M. Manalastas, A. Abu-Dayya, and A. Imran, "AI-Assisted RLF Avoidance for Smart EN-DC Activation," in *GLOBECOM 2020 - 2020 IEEE Global Communications Conference*, 2020, pp. 1–6.

[21] T. Bai and R. W. Heath, "Coverage and rate analysis for millimeter-wave cellular networks," *IEEE Transactions on Wireless Communications*, vol. 14, no. 2, pp. 1100–1114, 2015.

[22] M. Rebato, J. Park, P. Popovski, E. De Carvalho, and M. Zorzi, "Stochastic geometric coverage analysis in mmwave cellular networks with realistic channel and antenna radiation models," *IEEE Transactions on Communications*, vol. 67, no. 5, pp. 3736–3752, 2019.

[23] M. Di Renzo, "Stochastic geometry modeling and analysis of multi-tier millimeter wave cellular networks," *IEEE Transactions on Wireless Communications*, vol. 14, no. 9, pp. 5038–5057, 2015.

[24] J. Fan, L. Han, X. Luo, and J. Huang, "Delay analysis and optimization of beam scanning-based user discovery in millimeter wave systems," *IEEE Access*, vol. 8, pp. 25 075–25 083, 2020.

[25] C. Sun, J. Zhang, X. Zhang, and W. Wang, "Macro-assisted millimeter-wave small cell discovery in ultra dense wireless network," in *2017 IEEE International Conference on Internet of Things (iThings) and IEEE Green Computing and Communications (GreenCom) and IEEE Cyber, Physical and Social Computing (CPSCom) and IEEE Smart Data (SmartData)*, 2017, pp. 545–551.

[26] Y. J. Kim, H. Lee, and Y. S. Cho, "Beam-tracking technique for irs-assisted mmwave cellular systems with uniform planar array," *IEEE Transactions on Vehicular Technology*, vol. 72, no. 5, pp. 6844–6849, 2023.

[27] O. Onireti, A. Imran, and M. A. Imran, "Coverage analysis in the uplink of mmwave cellular networks," in *2017 European Conference on Networks and Communications (EuCNC)*, 2017, pp. 1–6.

[28] A. Taufique, A. Mohamed, H. Farooq, A. Imran, and R. Tafazolli, "Analytical modeling for mobility signalling in ultradense hetnets," *IEEE Transactions on Vehicular Technology*, vol. 68, no. 3, pp. 2709–2723, 2019.

[29] O. Onireti, A. Imran, M. A. Imran, and R. Tafazolli, "Energy efficient inter-frequency small cell discovery in heterogeneous networks," *IEEE Transactions on Vehicular Technology*, vol. 65, no. 9, pp. 7122–7135, 2016.

[30] O. Onireti, L. Zhang, A. Imran, and M. A. Imran, "Outage probability in the uplink of multitier millimeter wave cellular networks," *IEEE Systems Journal*, vol. 14, no. 2, pp. 2520–2531, 2020.

[31] H. N. Qureshi, A. Imran, and A. Abu-Dayya, "Enhanced MDT-Based Performance Estimation for AI Driven Optimization in Future Cellular Networks," *IEEE Access*, vol. 8, pp. 161 406–161 426, 2020.

[32] M. U. Bin Farooq, M. Manalastas, W. Raza, A. Ijaz, S. M. A. Zaidi, A. Abu-Dayya, and A. Imran, "Data driven optimization of inter-frequency mobility parameters for emerging multi-band networks," in *GLOBECOM 2020 - 2020 IEEE Global Communications Conference*, 2020, pp. 1–6.

[33] M. Manalastas, H. Farooq, S. M. Asad Zaidi, and A. Imran, "Where to go next?: A realistic evaluation of ai-assisted mobility predictors for hetnets," in *2020 IEEE 17th Annual Consumer Communications Networking Conference (CCNC)*, 2020, pp. 1–6.

[34] U. Masood, H. Farooq, and A. Imran, "A machine learning based 3d propagation model for intelligent future cellular networks," in *2019 IEEE Global Communications Conference (GLOBECOM)*, 2019, pp. 1–6.

[35] S. M. A. Zaidi, M. Manalastas, H. Farooq, and A. Imran, "SyntheticNET: A 3GPP Compliant Simulator for AI Enabled 5G and Beyond," *IEEE Access*, pp. 1–1, 2020.

Authorized licensed use limited to: University of Oklahoma Libraries. Downloaded on August 07,2023 at 17:17:36 UTC from IEEE Xplore. Restrictions apply.
© 2023 IEEE. Personal use is permitted, but republication/redistribution requires IEEE permission. See https://www.ieee.org/publications/rights/index.html for more information.

This article has been accepted for publication in IEEE Transactions on Vehicular Technology. This is the author's version which has not been fully edited and content may change prior to final publication. Citation information: DOI 10.1109/TVT.2023.3289718

[36] 3GPP, “3GPP TS 36.304 - Evolved Universal Terrestrial Radio Access (E-UTRA) User Equipment (UE) procedures in idle mode,” Tech. Rep., 2021.

[37] “everythingRF ksf410.a,” https://www.everythingrf.com/products/all-antennas/taoglas/741-318-ksf410-a, accessed: 2021-04-08.

[38] M. R. Akdeniz, Y. Liu, M. K. Samimi, S. Sun, S. Rangan, T. S. Rappaport, and E. Erkip, “Millimeter Wave Channel Modeling and Cellular Capacity Evaluation,” *IEEE Journal on Selected Areas in Communications*, vol. 32, no. 6, pp. 1164–1179, 2014.

[39] M. Pesko, T. Javornik, A. Kosir, M. Stular, and M. Mohorcic, “Radio environment maps: The survey of construction methods,” *KSII Transactions on Internet and Information Systems (TIIS)*, vol. 8, no. 11, pp. 3789–3809, 2014.

[40] J. Shodamola, H. Qureshi, U. Masood, and A. Imran, “Towards addressing the spatial sparsity of mdt reports to enable zero touch network automation,” in *2021 IEEE Global Communications Conference (GLOBECOM)*, 2021, pp. 1–6.

[41] M. S. Riaz, H. N. Qureshi, U. Masood, A. Rizwan, A. Abu-Dayya, and A. Imran, “A hybrid deep learning-based (hydra) framework for multifault diagnosis using sparse mdt reports,” *IEEE Access*, vol. 10, pp. 67 140–67 151, 2022.

[42] A. Rizwan, A. Abu-Dayya, F. Filali, and A. Imran, “Addressing data sparsity with gans for multi-fault diagnosing in emerging cellular networks,” in *2022 International Conference on Artificial Intelligence in Information and Communication (ICAIIC)*, 2022, pp. 318–323.

[43] “FAA GPS Performance Analysis Report,” National Transportation Safety Board, Tech. Rep., 2016. [Online]. Available: https://www.nstb.tc.faa.gov/REPORTS/PAN96_0117.pdf

[44] 3GPP, “37.863 - E-UTRA (Evolved Universal Terrestrial Radio Access) - NR Dual Connectivity (EN-DC) of LTE 1 Down Link (DL) / 1 Up Link (UL) and 1 NR band,” Tech. Rep., 2019.

Authorized licensed use limited to: University of Oklahoma Libraries. Downloaded on August 07,2023 at 17:17:36 UTC from IEEE Xplore. Restrictions apply.
© 2023 IEEE. Personal use is permitted, but republication/redistribution requires IEEE permission. See https://www.ieee.org/publications/rights/index.html for more information.